Polystibides

International Edition: DOI: 10.1002/anie.201510504
German Edition: DOI: 10.1002/ange.201510504

Synthesis and Structural Characterization of Magnesium-Substituted Polystibides $[(LMg)_4Sb_8]$

*Chelladurai Ganesamoorthy, Christoph Wölper, Anton S. Nizovtsev, and Stephan Schulz**

Dedicated to Professor Herbert W. Roesky on the occasion of his 80th birthday

Abstract: *Redox reactions of $[(L^{1,2}Mg)_2]$ and Sb_2R_4 (R = Me, Et) yielded the first Mg-substituted realgar-type Sb_8 polystibides $[(L^{1,2}Mg)_4(\mu_4,\eta^{2:2:2:2}\text{-}Sb_8)]$ (L^1 = HC[C(Me)N(2,4,6-$Me_3C_6H_2$)]$_2$, L^2 = HC[C(Me)N(2,6-i-$Pr_2C_6H_3$)]$_2$). Compounds $[(L^{1,2}Mg)_2]$ serve both as reducing agents, initiating the cleavage of the Sb–C bonds, and as stabilizers for the resulting Sb_8 polyanion. The polystibides were characterized by NMR and IR spectroscopies, elemental analysis, and X-ray structure analysis. In addition, results from quantum chemical calculations are presented.*

Compounds containing metal–metal bonds have attracted tremendous attention because of their fundamental appeal and their unique combination of properties, which facilitate their use in catalysis and small-molecule activation.[1] Spectacular examples of the d-block elements are the quadruple-bonded dianion $[Re_2Cl_8]^{2-}$ and the quintuple-bonded Cr^I dimer [Ar*CrCrAr*] (Ar* = 2,6-$(Dipp)_2C_6H_3$; Dipp = 2,6-diisopropylphenyl) as well as the dizincocene Cp*Zn-ZnCp* (Cp* = C_5Me_5) of Carmona and co-workers.[2] Inspired by this report, theoretical calculations predicted the existence of chemically relevant Mg^I dimers[3] and "bottleable" derivatives $[(L^{2,3}Mg)_2]$ (L^2 = HC[C(Me)N(Dipp)]$_2$, L^3 = (N^iPr_2)C{N(Dipp)}$_2$), which were reported in 2007 by Stasch et al.[4] Since then, the number of Mg^I dimers, which are typically stabilized by bulky, often chelating, organic ligands, has steadily increased.[5]

Mg^I compounds are soluble and selective two-electron reducing agents.[6] Their promising potential for the synthesis of unusual complexes was demonstrated in reduction reactions of carbodiimide, azobenzene, cyclooctatetraene, azides, isocyanates, CO_2, N_2O, and SO_2.[5a,7,8] In addition to their widespread reactivity toward small organic molecules, Mg^I dimers also function as "soft reductants" in the synthesis of low-valent p-block derivatives, in particular Group 13 and Group 14 elements.[9–14] The Mg^I dimers were found to exhibit superior behavior compared to traditional heterogeneous reductants, such as Na, K, and KC_8.

As part of our general interest in the chemistry of heavier Group 13/15 elements, we recently described reactions of Group 13 diyls L^2M (M = Al, Ga, In) with Et_3E and Et_4E_2 (E = Sb, Bi), which proceeded with insertion of L^2M into the E–C and E–E bonds and subsequent formation of L^2M-(Et)$BiEt_2$ and $L^2M(EEt_2)_2$.[15] The organic substituents at the E center were shown to have a subtle influence on the outcome of these reactions. A notable example is the reaction of L^2Ga and $Sb(NMe_2)_3$, which afforded a Ga-substituted distibene, $[L^2(Me_2N)GaSb{=}SbGa(NMe_2)L^2]$ and the first example of a Sb analogue of bicyclo[1.1.0]butane, $[\{L^2\text{-}(Me_2N)Ga\}_2Sb_4]$.[16] In this context, we now report the formation of $[(L^{1,2}Mg)_4Sb_8]$ (L^1 = HC[C(Me)N(2,4,6-$Me_3C_6H_2$)]$_2$ (**1**); L^2 = HC[C(Me)N(Dipp)]$_2$ (**2**)) from the reactions of Sb_2R_4 (R = Me, Et) with $[(L^{1,2}Mg)_2]$ (Scheme 1).

The reactions of Sb_2R_4 (R = Me, Et) with $[(L^{1,2}Mg)_2]$ in a 2:5 molar ratio, which are accompanied by gradual color changes from pale-yellow to red–orange, led to the formation of compounds **1** and **2** in 27–30% yield (Scheme 1). At ambient temperature, the reactions of Sb_2R_4 with $[(L^1Mg)_2]$ were complete after one day, whereas the reactions with the less reactive compound $[(L^2Mg)_2]$ required 3 days. In contrast, analogous reactions of Sb_2R_4 at 80 °C were finished after 4 h (employing $[(L^1Mg)_2]$) and 18 h ($[(L^2Mg)_2]$), respectively. Similar to the scrambling reaction of $L^2Ga(I)$ with Sb_2Et_4, which led to the insertion compound $[L^2Ga(SbEt_2)_2]$,[15b] the reaction may proceed with the initial formation of $L^{1,2}Mg$-SbR_2, which is then reduced by $[(L^{1,2}Mg)_2]$ to afford polystibides **1** and **2** as well as $L^{1,2}MgR$ (R = Me, Et). However, in situ NMR experiments provided no evidence for the formation of $L^{1,2}Mg$-SbR_2. The equimolar reaction of $[(L^{1,2}Mg)_2]$ and Sb_2Et_4 also did not produce $L^{1,2}Mg$-$SbEt_2$, instead only the formation of **1** and **2** and an excess of Sb_2Et_4 along with $L^{1,2}MgEt$ were detected in the ^1H NMR spectra. For the synthesis of **2**, Sb_2Me_4 was preferred over Sb_2Et_4 because of the poor solubility of L^2MgMe in aromatic solvents, which makes it easier to separate **2** from the reaction mixture. A similar reaction of $[(L^{1,2}Mg)_2]$ with Bi_2Et_4 at room temperature immediately resulted in the formation of a metallic mirror and $L^{1,2}MgEt$.

1 and **2**, which must be handled with care since they quickly turn into black precipitates upon exposure to traces of air and water, are stable in solution and in the solid state at

[*] Dr. C. Ganesamoorthy, Dr. C. Wölper, Prof. Dr. S. Schulz
Faculty of Chemistry, University of Duisburg-Essen
Universitätsstrasse 5–7, S07 S03 C30, 45117 Essen (Germany)
E-mail: stephan.schulz@uni-due.de
Dr. A. S. Nizovtsev
Nikolaev Institute of Inorganic Chemistry
Siberian Branch of the Russian Academy of Sciences
Academician Lavrentiev Avenue 3
630090, Novosibirsk (Russian Federation)
and
Novosibirsk State University
Pirogova Street 2, 630090, Novosibirsk (Russian Federation)

Supporting information for this article (including experimental details, ^1H and ^{13}C NMR and IR spectra, and computational details) can be found under http://dx.doi.org/10.1002/anie.201510504.

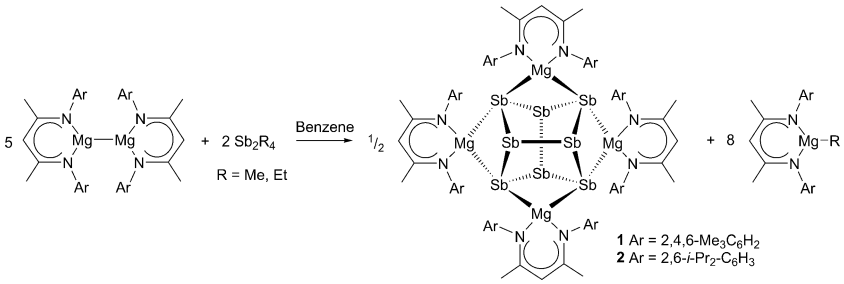

Scheme 1. Synthesis of **1** and **2**.

ambient temperature under an argon atmosphere in a glovebox. The compounds are sparingly soluble in benzene and toluene at ambient temperature, but dissolve well upon heating. The ^{1}H NMR spectrum of **1** in C_6D_6 shows eight resonance signals at ambient temperature. The C_2 rotation axis of ligand L^1 is lost by coordination to the Sb_8 moiety. Therefore, two sets of ^{1}H NMR resonance signals are detected compared to L^1H or $[(L^1Mg)_2]$ (see the sets of signals in the ^{1}H NMR spectra of **1**, L^1H, and $[(L^1Mg)_2]$ in the Supporting Information). Surprisingly, only one resonance signal at $\delta = 2.20$ ppm is detected for the *o*-CH_3 groups in the ^{1}H NMR spectrum, whereas two separate signals appear in the $^{13}C\{^1H\}$ NMR spectrum at 20.94 and 20.51 ppm. The $^{13}C\{^1H\}$ NMR spectrum of **1** at room temperature shows 17 signals including the characteristic resonances attributable to the γ-*C*H carbon atom ($\delta = 94.59$ ppm), the remaining two C_3N_2Mg ring carbon atoms (168.97, 168.23 ppm) as well as the methyl carbon atoms of the mesityl groups (22.59 (*p*-CH_3), 21.99 (*p*-CH_3), 20.94 (*o*-CH_3), 20.51 (*o*-CH_3) ppm) and the two α-substituents (23.76, 23.57 ppm). The remaining signals are from the phenyl carbon atoms (144.97, 144.06, 133.97, 133.50, 132.35, 131.79, 130.60 (*m*-C), 130.46 (*m*-C) ppm).

^{1}H and $^{13}C\{^1H\}$ NMR spectral patterns of **2** are similar to **1**. The ^{1}H NMR spectrum of **2** in [D_8]toluene exhibits single resonance signals for the γ-H and two methyl groups of the C_3N_2Mg ring at $\delta = 4.74$, 1.60, and 1.54 ppm, respectively. The methyl protons of the isopropyl substituents broaden from 1.50 to 0.95 ppm, whereas the methine protons appear as a two overlapping septets at $\delta = 2.99$ ppm. Similar broad signals have also been detected in the aromatic and aliphatic regions of **2** in the $^{13}C\{^1H\}$ NMR spectrum, however, the observed signals are consistent with the characteristic resonance signals of the organic substituents. Although **1** and **2** could be reproducibly isolated in pure form from both reactions, additional signals were detected in the ^{1}H NMR spectra of the crude reaction mixtures. Unfortunately, to date all efforts to isolate the other components of the reaction mixture have been unsuccessful.

Crystals of **1** and **2** were obtained from saturated benzene solutions at ambient temperature after storage for several days.[17] **1** crystallizes in the triclinic space group $P\bar{1}$. In the molecular structure of **1**, the unit cell consists of two independent molecules with almost identical conformations and structural parameters. One of these independent molecules is depicted in Figure 1 and is described below. Compound **2** crystallizes in the tetragonal space group *P*4/*ncc* with the molecule placed on Wyckoff-position 4a. The 2.22 symmetry of this position leads to a quarter of the molecule forming the asymmetric unit. The crystals of **2** showed severe degradation of quality and signs of modulation upon cooling to 100 K. Therefore, the crystal was measured at 200 K. The quality of the resulting model is still limited but good enough to give a realistic view of the connectivity, although quantitative results should be carefully accessed (see Figure S16 in the Supporting Information).

The structures of **1** and **2** each consist of a Sb_8 unit stabilized by four chelating $L^{1,2}Mg$ moieties. Each Mg center is fourfold-coordinated by a chelating β-diketiminate ligand and two Sb atoms with distorted tetrahedral geometry. The mean Mg–N bond lengths (**1**: 2.026 Å; **2**: 2.063 Å) within the almost planar C_3N_2Mg heterocycles of **1** and **2** are comparable to those reported for β-diketiminate magnesium complexes with fourfold-coordinated Mg atoms, such as $L^1MgI(OEt_2)$ (2.031(2), 2.036(2) Å), $L^1MgI(THF)$ (2.026(2), 2.036(2) Å), $[(L^1MgI)_2]$ (2.004(2), 2.001(2) Å), and $[(L^1MgH)_2]$ (2.0219(14), 2.0226(13) Å), and to those reported for $(L^1)_2Mg$ (2.0796(17), 2.0579(17), 2.0738(17) Å).[5c,10c] The Mg–Sb bond lengths of **1** (2.8459(10)–2.9007(10) Å) are

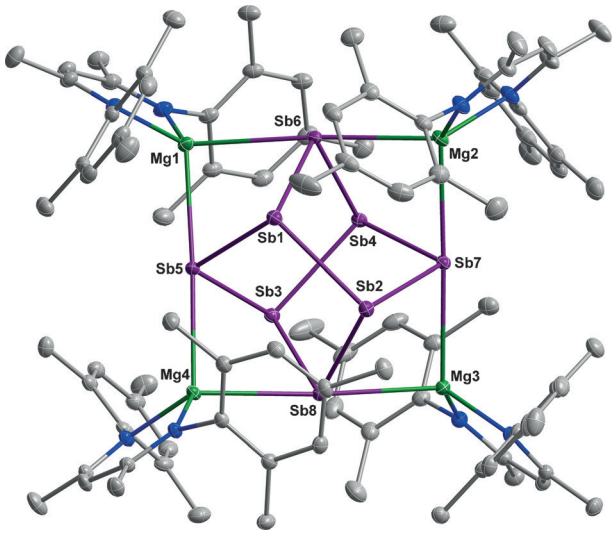

Figure 1. Molecular structure of $[(L^1Mg)_4Sb_8]$ (**1**). H atoms have been omitted for clarity and displacement ellipsoids are set at 30% probability. Selected bond lengths [Å] and angles [°]: Mg1–Sb5 2.8459(10), Mg1–Sb6 2.9007(10), Mg2–Sb6 2.8958(11), Mg2–Sb7 2.8603(10), Mg3–Sb7 2.8627(9), Mg3–Sb8 2.8663(10), Mg4–Sb5 2.8521(9), Mg4–Sb8 2.8855(10), Sb1–Sb2 2.8580(4), Sb1–Sb5 2.8130(4), Sb1–Sb6 2.8113(4), Sb2–Sb7 2.7974(4), Sb2–Sb8 2.8209(4), Sb3–Sb4 2.8582(4), Sb3–Sb5 2.8083(4), Sb3–Sb8 2.8082(4), Sb4–Sb6 2.8174(4), Sb4–Sb7 2.8056(4); Sb5-Mg1-Sb6 87.43(3), Sb6-Mg2-Sb7 87.69(3), Sb7-Mg3-Sb8 88.68(3), Sb5-Mg4-Sb8 87.07(3), Sb1-Sb5-Sb3 101.109(12), Sb1-Sb6-Sb4 99.422(10), Sb2-Sb7-Sb4 100.821(11), Sb2-Sb8-Sb3 99.378(10), Mg1-Sb6-Mg2 174.45(3), Mg2-Sb7-Mg3 178.17(3), Mg3-Sb8-Mg4 175.40(3), Mg1-Sb5-Mg4 177.32(3). Data for the second independent molecule are given in the cif file. Atom colors: N = blue; C = gray.

slightly shorter compared to those of **2** (2.882(3)–3.007(3) Å), but for both compounds the sum of the covalent radii (Mg = 1.39 Å; Sb = 1.40 Å) is slightly exceeded.[18] The Sb-Mg-Sb angles of **1** (87.07(3)–88.68(3)°) and **2** (84.76(8)°) are similar. The only structurally characterized magnesium stibide, $[\{Me_2SiSi(SiMe_3)_2\}_2SbMgBr(OEt_2)_2]$, shows a slightly shorter Mg–Sb bond length of 2.7806(13) Å.[19] The eight Sb atoms in **1** can be divided into tricoordinated (Sb′) and tetracoordinated (Sb″) atoms (Figure 2). The Mg-Sb″-Mg units are

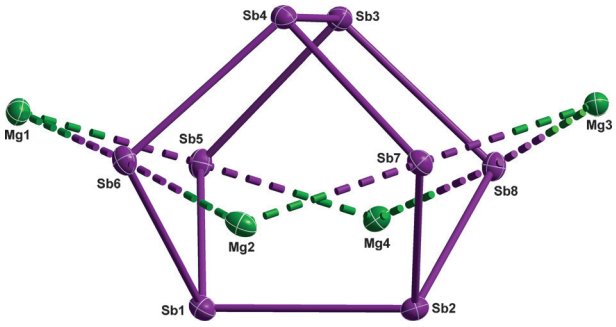

Figure 2. Mg_4Sb_8 skeleton of **1**. L^1 ligands are omitted for clarity, ellipsoids are set at 30% probability level.

almost linear (174.45(3)–178.17(3)°), whereas the butterfly-shaped $Mg_4Sb''_4$ unit has a dihedral angle of 29.35° (Mg1-Mg4-Mg3-Mg2). The angles within the Sb_8 cluster of **1** range from 89.449(11)° to 103.226(11)° and the Sb–Sb distances range from 2.7974(4) Å to 2.8582(4) Å, which is in good agreement with those detected in $\{(Me_3Si)_2CH\}_4Sb_8$ (2.784(4)–2.86184) Å).[20] Note that the Sb′1–Sb′2 (2.8580-(4) Å) and Sb′3–Sb′4 (2.8582(4) Å) distances of **1** are slightly longer than the Sb′–Sb″ bonds, which range from 2.7974(4) to 2.8209(4) Å (molecule 1). These results are comparable to those obtained for **2**, which also shows a long Sb′–Sb″ bond (2.8616(12) Å) and shorter Sb′–Sb″ bonds (2.7820(8)–2.8084(7) Å).

The solid-state structures of **1** and **2** are very similar to those of analogous polyphosphides, such as $[(L_2M)_4P_8]$ (L = Cp*, M = Sm; L_2 = 1,1′-fc(NSi^{t}BuMe$_2$)$_2$, M = Sc, fc = ferrocenyl),[21] which were obtained from redox reactions of white phosphorous P_4 with divalent Cp^*_2Sm or the scandium naphthalene complex $[(1,1'\text{-fc}(NSi^tBuMe_2)_2)Sc]_2(\mu\text{-}C_{10}H_8)$,[22] and are also similar to those of $Cp'_4Fe_4(CO)_6P_8$, $Cp'_4Fe_6(CO)_{13}P_8$ ($Cp' = \eta^5\text{-}C_5H_4Me$),[23] and alkyl-substituted P_8R_4 clusters.[24] Since the dimerization of two P_4 molecules to form a P_8 unit is enthalpically disfavored,[25] their formation was explained by electron transfer from the reducing agent to the P_4 molecule, subsequently yielding tetraanionic polyphosphides P_8^{4-}, which adopt realgar-type structures, also called an α-P_8 structure. According to quantum chemical calculations, the neutral P_8 molecule should adopt the cuneane structure, which shows two additional P–P bonds compared to the α-P_8 structure and which are replaced by four lone pairs in the polyphosphides.[26]

In analogy to these phosphorus compounds, the central Sb_8 unit in **1** and **2**, which also adopt the realgar-type homoatomic structure, can be described as an Sb_8^{4-} unit (Figure 2). Even though homoatomic Zintl-type polystibides, including Sb_4^{2-}, Sb_5^{5-}, Sb_7^{3-}, and Sb_{11}^{3-}, are well known,[27] to the best of our knowledge, **1** and **2** are the first examples containing a $[Sb_8]^{4-}$ polyanion. However, Korber and Reil reported the structure of a $[Sb_8]^{8-}$ Zintl anion, which adopts a ring structure as detected for S_8.[28] In addition, Breunig et al. synthesized the polystibine $Sb_8[CH(SiMe_3)_2]_4$, a metal–organic derivative containing a Sb_8 core analogous to that detected for **1** and **2**, by reduction of $(SiMe_3)_2HCSbCl_2$ with Mg,[20] whereas von Hänisch and Nikolova successfully prepared $[Sb_4(PSiMe_2Thex)_4]$ (Thex = $CMe_2{}^iPr$) and $[Sb_4(AsSi^iPr_3)_4]$ with central Sb_4E_4 (E = P, As) realgar-type core structures.[29] The Sb–Sb bond lengths in $[Sb_4(PSiMe_2Thex)_4]$ (2.879 Å) and $[Sb_4(AsSi^iPr_3)_4]$ (2.881–2.890 Å) are slightly elongated compared to those in **1**.

Very recently, Roesky et al. reported the first examples of Sm-substituted polyarsenides $[(Cp''_2Sm)(\mu,\eta^4{:}\eta^4\text{-}As_4)(Cp^*Fe)]$ and $[(Cp''_2Sm)_2As_7(Cp^*Fe)]$ ($Cp'' = \eta^5$-1,3-(tBu)$_2C_5H_3$) from the redox reactions of $[Cp^*Fe(\eta^5\text{-}As_5)]$ and $[Cp''_2Sm(thf)]$. $[(Cp''_2Sm)(\mu,\eta^4{:}\eta^4\text{-}As_4)(Cp^*Fe)]$ is the first d/f-triple decker sandwich complex containing a central As_4^{2-} unit, whereas $[(Cp''_2Sm)_2As_7(Cp^*Fe)]$ consists of a norbornadiene-type As_7^{3-} cage structural motif.[30a] $[L^2Mg^nBu]$ is also known to activate white phosphorus and afforded the dianions $[^nBu_2P_4]^{2-}$ and $[^nBu_2P_8]^{2-}$ from 2:1 and 1:1 molar reactions of P_4 and $[L^2Mg^nBu]$.[30b] Additionally, a cuneane-type complex $[Cp^*IrCO]_2\text{-}P_8[Cr(CO)_5]_3$ was obtained by reaction of white phosphorus with $[Cp^*Ir(CO)_2]$ under thermal and photochemical conditions.[30c]

To gain further insight into the interatomic interactions, electronic structure calculations were performed for **1** with an emphasis on the bonding situation in the Mg_4Sb_8 skeleton (Figure 3 a).[31]

BP86-D3BJ/def2-SVP computation[32] converged to a D_2-symmetrical structure for $[(L^1Mg)_4Sb_8]$. The calculated geometric parameters agree well with the experimental values (deviations from experimental bond lengths range from 0.03 to 0.08 Å for the Mg_4Sb_8 core). The $(L^1Mg)^+$ moiety was found to bind rather strongly to $[(L^1Mg)_3Sb_8]^-$ (ΔG°_{298} = 136.9 kcal mol^{-1}; Table S1). The ΔG°_{298} value for the dissociation of $[(L^1Mg)_4Sb_8]$ into four $(L^1Mg)^+$ and one $[Sb_8]^{4-}$ ions is equal to 989.4 kcal mol^{-1} at the B3LYP-D3BJ/def2-TZVP//BP86-D3BJ/def2-SVP level of theory (Table S1).[33] According to the energy decomposition analysis (EDA; Table S2),[34] electrostatic interactions (ΔE_{elstat}, 44 %) between $(L^1Mg)^+$ and $[(L^1Mg)_3Sb_8]^-$ dominate over orbital interactions (ΔE_{orb}, 32 %). It is important to note that the dispersion term (ΔE_{disp}, 24 %) also gives a noticeable contribution to the total attractive interactions. Computed atoms in molecules (AIM) parameters (Table S3) indicate an intermediate character for the Mg–Sb and Sb–Sb bonds ($\nabla^2\rho(\mathbf{r}_b) > 0$; $1 < |V(\mathbf{r}_b)|/G(\mathbf{r}_b) < 2$, $H(\mathbf{r}_b) < 0$).[35] However, the Mg–Sb bonds have a high ionic contribution, whereas the Sb–Sb bonds are rather covalent, as can be seen from the corresponding values for the AIM parameters. Natural population analysis (NPA) partial charges on Mg and Sb ($+1.16\,|e|$ versus $-0.54/-0.55\,|e|$; Table S3) imply highly polarized Mg–Sb bonds. Additionally, natural bond orbital analysis (NBO)[36] reveals no covalent Mg–Sb bonds, which is in line

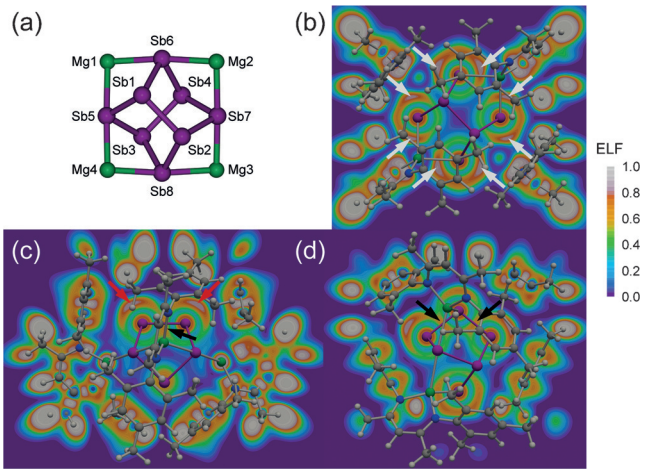

Figure 3. a) Atomic labeling for the Mg_4Sb_8 skeleton and b–d) ELF distribution in the $[(L^1Mg)_4Sb_8]$ complex in the b) Sb5-Sb6-Sb7, c) Mg1-Sb1-Sb2, and d) Sb4-Sb7-Sb2 planes. V(Mg,Sb), V(Sb), and V(Sb,Sb) basins are indicated by white (b), red (c), and black (c, d) arrows.

with results of quantum chemical calculations on a Li_4Sb_8 cluster with a realgar-type $[Sb_8]^{4-}$ skeleton,[37] for which ionic interactions between the Li and Sb atoms were found. The chemical bonding pattern for the Sb_8 fragment in $[(L^1Mg)_4Sb_8]$ complex is analogous to the $[Sb_8]^{4-}$ core of the Li_4Sb_8 cluster.[37] The pattern includes eight s-type lone pairs (occupation number (ON) = 1.9 | *e* | for Sb1, Sb2, Sb3, Sb4; ON = 1.7 | *e* | for Sb5, Sb6, Sb7, Sb8), four p-type lone pairs (ON = 1.9 | *e* |), and ten covalent two-center two-electron Sb–Sb bonds (ON = 1.9 | *e* |). Electron localization function (ELF)[38] (Figure 3b) reveals eight valence basins between Mg and Sb atoms with a population of 2.5 *e* (Table S3), indicating some degree of covalent bonding. However, these V(Mg,Sb) basins are displaced from the corresponding bond lines, which is not typical for covalent bonds. Moreover, the Mg atoms contribute only 0.1 *e* into the V(Mg,Sb) basin, as calculated by an ELF/AIM intersection procedure (Table S3).[39] Thus, these objects can be attributed to the lone pairs of Sb [V(Mg,Sb) ≈ V(Sb)]. As shown in Figure 3c, each inner Sb atom (Sb1, Sb2, Sb3, Sb4) has one V(Sb) valence monosynaptic basin populated by 2.7 *e*, which is associated with the lone pair localized on Sb. The presence of V(Sb,Sb) basins ($\overline{N}$[V(Sb,Sb)] = 1.4–1.6 *e*; Figures 3c,d) suggests a covalent bonding between these atoms. Thus, on the basis of the AIM, EDA, ELF, and NBO analyses it can be concluded that the Sb–Sb bonds are covalent, whereas the Mg–Sb bonds have a mixed character with a dominant ionic contribution. In other words, bonds between Mg and Sb atoms can be described as highly polar covalent.

In summary, the first magnesium polystibides containing realgar-type clusters of the general type $[(L^{1,2}Mg)_4Sb_8]$ were obtained in two-centered/two-electron reduction reactions of $[(L^{1,2}Mg)_2]$ with Sb_2R_4 (R = Me, Et). In spite of their different steric environments, both mesityl and diisopropylphenyl derivatives of $[(L^{1,2}Mg)_2]$ gave rise to the formation of similar clusters. Compounds **1** and **2** are presumably the orthogonally fused version of the two bicyclo[1.1.0]butane-type Sb_4 units. Dimerizations of this type have also been detected in As derivatives. For example, stirring the solution of $[\{Cp^*Cr(CO)_3\}_2(\mu,\eta^{1:1}\text{-}As_4)]$ under ambient conditions led to the formation of $[\{Cp^*Cr(CO)_3\}_4(\mu_4,\eta^{1:1:1:1}\text{-}As_8)]$. Similarly, irradiation of $[\{Cp'''Fe(CO)_2\}_2(\mu,\eta^{1:1}\text{-}As_4)]$ ($Cp''' = 1,2,4\text{-}(^tBu)_3C_5H_2$) for two hours with UV light produced $[\{Cp'''Fe(CO)_2\}_2\{Cp'''Fe(CO)\}_2(\mu_4,\eta^{1:1:2:2}\text{-}As_8)]$.[40] We are currently looking into the possibility to synthesize smaller aggregates (Sb < 8), such as the hypothetical molecules $L^{1,2}MgSb=SbMgL^{1,2}$, $(L^{1,2}Mg)_2Sb_4$, and $(L^{1,2}Mg)_3Sb_7$, which would give an insight into the formation of polynuclear aggregates from simple monomers in such redox reactions.[16] The use of $[(L^{1,2}Mg)_2]$ compounds as facile two-electron reductants toward other heavier main-group elements may offer opportunities to prepare unprecedented molecules and clusters stabilized by LMg^+ units.

Experimental Section

^1H and ^{13}C NMR and IR spectra of **1** and **2** as well as quantum chemical details are provided in the Supporting Information.

Synthesis of **1**: A mixture of $[(L^1Mg)_2]$ (0.492 g, 0.688 mmol) and Sb_2Et_4 (0.099 g, 60 μL, 0.275 mmol) was dissolved in 1 mL of benzene and heated at 80 °C for 4 h. The reaction mixture was cooled to ambient temperature and the red solution was separated from the white precipitate L^1MgEt. Storage of the red solution at room temperature for 5 days yielded red crystals of **1**. Yields: **1**: 50 mg (0.0208 mmol, 30 %); L^1MgEt: 0.404 g (1.044 mmol, 95 %). Elemental analysis calcd. (%) for $C_{92}H_{116}N_8Mg_4Sb_8$: C 45.94, H 4.86, N 4.66; found: C 46.10, H 4.80, N 4.70. IR (neat): $\tilde{\nu}$ = 3001, 2911, 2849, 1544, 1522, 1443, 1375, 1263, 1190, 1145, 1010, 954, 920, 853, 824, 740, 627, 565, 498 cm^{-1}. ^1H NMR (C_6D_6, 300 MHz, 25 °C): δ = 7.11 (s, 2H, $C_6H_2(Me)_3$), 7.04 (s, 2H, $C_6H_2(Me)_3$), 4.79 (s, 1H, γ-C*H*-), 2.73 (s, 3H, *p*-CH_3), 2.56 (s, 3H, *p*-CH_3), 2.20 (s, 12H, *o*-CH_3), 1.66 (s, 3H, ArNCCH_3), 1.61 ppm (s, 3H, ArNCCH_3). $^{13}C\{^1H\}$ NMR (C_6D_6, 75.5 MHz, 25 °C): δ = 168.97, 168.23 (ArN*C*CH_3), 144.97, 144.06, 133.97, 133.50, 132.35, 131.79, 130.60 (*m*-C), 130.46 (*m*-C) (C_6H_2), 94.59 (γ-*C*H-), 23.76, 23.57 (ArNC*C*H_3), 22.59 (*p*-*C*H_3), 21.99 (*p*-*C*H_3), 20.94 (*o*-*C*H_3), 20.51 ppm (*o*-*C*H_3).

Synthesis of **2**: $[(L^2Mg)_2]$ (0.746 g, 0.844 mmol) was suspended in 10 mL of fluorobenzene and Sb_2Me_4 (0.102 g, 50 μL, 0.338 mmol) was added. The reaction mixture was stirred at 80 °C for 18 h. The resulting red solution was separated from the white precipitate L^2MgMe and was stored at RT for 15 days to afford analytically pure red crystals of **2**. The manipulation of the reaction products was performed inside a glove box to avoid forming the black precipitate. Yield: **2**: 62.4 mg (0.0228 mmol, 27 %); L^2MgMe: 0.565 g (1.236 mmol, 92 %). Elemental analysis calcd. (%) for $C_{116}H_{164}N_8Mg_4Sb_8$: C 50.81, H 6.03, N 4.09; Found: C 50.90, H 6.08, N 4.15. IR (neat): $\tilde{\nu}$ = 2959, 2924, 2863, 1520, 1393, 1309, 1255, 1177, 1099, 1021, 925, 847, 787, 757, 703, 619, 523, 487, 445 cm^{-1}. ^1H NMR ([D_8]toluene, 300 MHz, 25 °C): δ = 7.30–7.14 (m, 6H, $C_6H_3(^iPr)_2$), 4.74 (s, 1H, γ-C*H*-), 2.99 (two sept, 4H, -C*H*(CH_3)$_2$), 1.60 (s, 3H, ArNCCH_3), 1.54 (s, 3H, ArNCCH_3), 1.50–0.95 ppm (br m, 24H, -CH(CH_3)$_2$). $^{13}C\{^1H\}$ NMR (D_8]toluene, 150 MHz, 25 °C): δ = 169.67, 169.65 (ArN*C*CH_3), 146.40, 145.36, 143.00, 126.28, 126.24, 125.13 (C_6H_3), 96.25 (γ-*C*H-), 28.26 (br s, -*C*H(CH_3)$_2$), 25.99, 25.63 (ArNC*C*H_3), 25.61, 25.17 (br s), 21.33 ppm (-CH(*C*H_3)$_2$).

Acknowledgements

S.S. gratefully acknowledges financial support by the University of Duisburg-Essen. A.S.N. acknowledges the Russian

Science Foundation for financial support (Grant No. 14-23-00013). The Siberian Supercomputer Center is gratefully acknowledged for providing computational resources.

Keywords: cluster compounds · main group elements · metal–metal interactions · subvalent compounds

How to cite: *Angew. Chem. Int. Ed.* **2016**, *55*, 4204–4209
Angew. Chem. **2016**, *128*, 4276–4281

[1] For example, see: a) F. A. Cotton, C. A. Murillo, R. A. Walton, *Multiple Bonds Between Metal Atoms*, 3rd ed., Springer, New York, **2005**; b) J. F. Berry, *J. Chem. Sci.* **2015**, *127*, 209–214; c) J. P. Krogman, C. M. Thomas, *Chem. Commun.* **2014**, *50*, 5115–5127; d) B. G. Cooper, J. W. Napoline, C. M. Thomas, *Catal. Rev. Sci. Eng.* **2012**, *54*, 1–40; e) C. M. Thomas, *Comments Inorg. Chem.* **2011**, *32*, 14–38; f) J. P. Collman, R. Boulatov, *Angew. Chem. Int. Ed.* **2002**, *41*, 3948–3961; *Angew. Chem.* **2002**, *114*, 4120–4134.

[2] a) T. Nguyen, A. D. Sutton, M. Brynda, J. C. Fettinger, G. J. Long, P. P. Power, *Science* **2005**, *310*, 844–847; b) I. Resa, E. Carmona, E. Gutierrez-Puebla, A. Monge, *Science* **2004**, *305*, 1136–1138; c) F. A. Cotton, N. F. Curtis, C. B. Harris, B. F. G. Johnson, S. J. Lippard, J. T. Mague, W. R. Robinson, J. S. Wood, *Science* **1964**, *145*, 1305–1307.

[3] a) M. Westerhausen, M. Gärtner, R. Fischer, J. Langer, L. Yu, M. Reiher, *Chem. Eur. J.* **2007**, *13*, 6292–6306; b) A. Velazquez, I. Fernández, G. Frenking, G. Merino, *Organometallics* **2007**, *26*, 4731–4736; c) Q. S. Li, Y. Xu, *J. Phys. Chem. A* **2006**, *110*, 11898–11902; d) Y. Xie, H. F. Schaefer III, E. D. Jemmis, *Chem. Phys. Lett.* **2005**, *402*, 414–421; e) P. G. Jasien, C. E. Dykstra, *J. Am. Chem. Soc.* **1985**, *107*, 1891–1895; f) P. G. Jasien, C. E. Dykstra, *Chem. Phys. Lett.* **1984**, *106*, 276–279.

[4] S. P. Green, C. Jones, A. Stasch, *Science* **2007**, *318*, 1754–1757.

[5] a) A. J. Boutland, I. Pernik, A. Stasch, C. Jones, *Chem. Eur. J.* **2015**, *21*, 15749–15758; b) A. Stasch, *Angew. Chem. Int. Ed.* **2014**, *53*, 10200–10203; *Angew. Chem.* **2014**, *126*, 10364–10367; c) S. J. Bonyhady, C. Jones, S. Nembenna, A. Stasch, A. J. Edwards, G. J. McIntyre, *Chem. Eur. J.* **2010**, *16*, 938–955; d) Y. Liu, S. Li, X.-J. Yang, P. Yang, B. Wu, *J. Am. Chem. Soc.* **2009**, *131*, 4210–4211; e) S. P. Green, C. Jones, A. Stasch, *Angew. Chem. Int. Ed.* **2008**, *47*, 9079–9083; *Angew. Chem.* **2008**, *120*, 9219–9223.

[6] a) C. Jones, A. Stasch, *Top. Organomet. Chem.* **2013**, *45*, 73–101; b) A. Stasch, C. Jones, *Dalton Trans.* **2011**, *40*, 5659–5672.

[7] S. J. Bonyhady, S. P. Green, C. Jones, S. Nembenna, A. Stasch, *Angew. Chem. Int. Ed.* **2009**, *48*, 2973–2977; *Angew. Chem.* **2009**, *121*, 3017–3021.

[8] a) C. E. Kefalidis, A. Stasch, C. Jones, L. Maron, *Chem. Commun.* **2014**, *50*, 12318–12321; b) R. Lalrempuia, A. Stasch, C. Jones, *Chem. Sci.* **2013**, *4*, 4383–4388.

[9] S. L. Choong, C. Schenk, A. Stasch, D. Dange, C. Jones, *Chem. Commun.* **2012**, *48*, 2504–2506.

[10] a) C. Jones, A. Sidiropoulos, N. Holzmann, G. Frenking, A. Stasch, *Chem. Commun.* **2012**, *48*, 9855–9857; b) N. Holzmann, A. Stasch, C. Jones, G. Frenking, *Chem. Eur. J.* **2011**, *17*, 13517–13525; c) S. J. Bonyhady, D. Collis, G. Frenking, N. Holzmann, C. Jones, A. Stasch, *Nat. Chem.* **2010**, *2*, 865–869; d) A. Sidiropoulos, C. Jones, A. Stasch, S. Klein, G. Frenking, *Angew. Chem. Int. Ed.* **2009**, *48*, 9701–9704; *Angew. Chem.* **2009**, *121*, 9881–9884.

[11] T. J. Hadlington, C. Jones, *Chem. Commun.* **2014**, *50*, 2321–2323.

[12] C. Jones, S. J. Bonyhady, N. Holzmann, G. Frenking, A. Stasch, *Inorg. Chem.* **2011**, *50*, 12315–12325.

[13] W. D. Woodul, E. Carter, R. Müller, A. F. Richards, A. Stasch, M. Kaupp, D. M. Murphy, M. Driess, C. Jones, *J. Am. Chem. Soc.* **2011**, *133*, 10074–10077.

[14] H. Braunschweig, A. Damme, R. D. Dewhurst, A. Vargas, *Nat. Chem.* **2013**, *5*, 115–121.

[15] a) C. Ganesamoorthy, D. Bläser, C. Wölper, S. Schulz, *Organometallics* **2015**, *34*, 2991–2996; b) C. Ganesamoorthy, D. Bläser, C. Wölper, S. Schulz, *Angew. Chem. Int. Ed.* **2014**, *53*, 11587–11591; *Angew. Chem.* **2014**, *126*, 11771–11775; c) C. Ganesamoorthy, D. Bläser, C. Wölper, S. Schulz, *Chem. Commun.* **2014**, *50*, 12382–12384.

[16] L. Tuscher, C. Ganesamoorthy, D. Bläser, C. Wölper, S. Schulz, *Angew. Chem. Int. Ed.* **2015**, *54*, 10657–10661; *Angew. Chem.* **2015**, *127*, 10803–10807.

[17] The crystals were mounted on nylon loops in inert oil. Data were collected on a Bruker AXS D8 Kappa diffractometer with APEX2 detector (monochromated $Mo_{K\alpha}$ radiation, $\lambda = 0.71073$ Å). The structures were solved by direct methods (SHELXS-97; G. M. Sheldrick, *Acta Crystallogr. Sect. A* **1990**, *46*, 467) and refined anisotropically by full-matrix least-squares on F^2 (SHELXL-2014; G. M. Sheldrick, *Acta Crystallogr. Sect. A* **2008**, *64*, 112 and shelXle, C. B. Hübschle, G. M. Sheldrick, B. Dittrich, *J. Appl. Crystallogr.* **2011**, *44*, 1281). Absorption corrections were performed semiempirically from equivalent reflections on the basis of multi-scans (Bruker AXS APEX2). Hydrogen atoms were refined using a riding model or rigid methyl groups. **1**: $[C_{92}H_{116}Mg_4N_8Sb_8]$, $M = 2405.16$, orange crystal, $(0.184 \times 0.166 \times 0.076$ mm); triclinic, space group $P\bar{1}$; $a = 15.3947(18)$, $b = 21.451(3)$, $c = 30.779(4)$ Å; $\alpha = 98.574(6)$, $\beta = 102.194(6)$, $\gamma = 95.022(6)°$; $V = 9749(2)$ Å^3; $Z = 4$; $\mu = 2.253$ mm^{-1}; $\rho_{calc} = 1.639$ g cm^{-3}; 260201 reflections, ($\theta_{max} = 33.338°$), 73624 unique ($R_{int} = 0.0371$); 2081 parameters; largest max./min. in the final difference Fourier synthesis 1.696 e Å^{-3}/−1.021 e Å^{-3}; max./min. transmission 0.40/0.50; $R1 = 0.0337$ ($I > 2\sigma(I)$), $wR2 = 0.0878$ (all data). **2**: $[C_{116}H_{164}Mg_4N_8Sb_8]$, $M = 2741.78$, orange crystal, $(0.444 \times 0.090 \times 0.075$ mm); tetragonal, space group $P4/ncc$; $a = 24.3186(7)$, $b = 24.3186(7)$, $c = 25.7075(7)$ Å; $\alpha = 90$, $\beta = 90$, $\gamma = 90°$; $V = 15203.3(10)$ Å^3; $Z = 4$; $\mu = 1.453$ mm^{-1}; $\rho_{calc} = 1.198$ g cm^{-3}; 161781 reflections, ($\theta_{max} = 30.576°$), 11652 unique ($R_{int} = 0.0729$); 318 parameters; largest max./min. in the final difference Fourier synthesis 4.740 e Å^{-3}/−1.745 e Å^{-3}; max./min. transmission 0.59/0.75; $R1 = 0.0986$ ($I > 2\sigma(I)$), $wR2 = 0.3485$ (all data). CCDC 1436397 (**1**) and 1448391 (**2**) contain the supplementary crystallographic data for this paper. These data can be obtained free of charge from The Cambridge Crystallographic Data Centre.

[18] P. Pyykkö, M. Atsumi, *Chem. Eur. J.* **2009**, *15*, 186–197.

[19] R. Zitz, J. Baumgartner, C. Marschner, *Organometallics* **2015**, *34*, 1431–1439.

[20] a) G. Balázs, H. J. Breunig, E. Lork, S. Mason, *Organometallics* **2003**, *22*, 576–585; b) H. J. Breunig, R. Rösler, E. Lork, *Angew. Chem. Int. Ed. Engl.* **1997**, *36*, 2237–2238; *Angew. Chem.* **1997**, *109*, 2333–2334.

[21] T. Li, S. Kaercher, P. W. Roesky, *Chem. Soc. Rev.* **2014**, *43*, 42–57.

[22] a) W. Huang, P. L. Diaconescu, *Chem. Commun.* **2012**, *48*, 2216–2218; b) S. N. Konchenko, N. A. Pushkarevsky, M. T. Gamer, R. Köppe, H. Schnöckel, P. W. Roesky, *J. Am. Chem. Soc.* **2009**, *131*, 5740–5741.

[23] M. E. Barr, B. R. Adams, R. R. Weller, L. E. Dahl, *J. Am. Chem. Soc.* **1991**, *113*, 3052–3060.

[24] a) C. P. Butts, M. Green, T. N. Hooper, R. J. Kilby, J. E. McGrady, D. A. Pantazis, C. A. Russell, *Chem. Commun.* **2008**, 856–858; b) M. Baudler, B. Koll, C. Adamek, R. Gleiter, *Angew. Chem. Int. Ed. Engl.* **1987**, *26*, 347–348; *Angew. Chem.* **1987**, *99*, 371–372.

[25] R. Ahlrichs, S. Brode, C. Ehrhardt, *J. Am. Chem. Soc.* **1985**, *107*, 7260 – 7264.
[26] B. M. Gimarc, D. S. Warren, *Inorg. Chem.* **1993**, *32*, 1850 – 1856.
[27] For a review, see: S. Scharfe, F. Kraus, S. Stegmaier, A. Schier, T. F. Fässler, *Angew. Chem. Int. Ed.* **2011**, *50*, 3630 – 3670; *Angew. Chem.* **2011**, *123*, 3712 – 3754.
[28] M. Reil, N. Korber, *Z. Anorg. Allg. Chem.* **2007**, *633*, 1599 – 1602.
[29] D. Nikolova, C. von Hänisch, *Eur. J. Inorg. Chem.* **2005**, 378 – 382.
[30] a) N. Arleth, M. T. Gamer, R. Köppe, S. N. Konchenko, M. Fleischmann, M. Scheer, P. W. Roesky, *Angew. Chem. Int. Ed.* **2016**, *55*, 1557 – 1560; *Angew. Chem.* **2016**, *128*, 1583 – 1586; b) M. Arrowsmith, M. S. Hill, A. L. Johnson, G. Kociok-Köhn, M. F. Mahon, *Angew. Chem. Int. Ed.* **2015**, *54*, 7882 – 7885; *Angew. Chem.* **2015**, *127*, 7993 – 7996; c) M. Scheer, U. Becker, E. Matern, *Chem. Ber.* **1996**, *129*, 721 – 724.
[31] Complete computational details are given in the Supporting Information.
[32] a) A. D. Becke, *Phys. Rev. A* **1988**, *38*, 3098 – 3100; b) J. P. Perdew, *Phys. Rev. B* **1986**, *33*, 8822 – 8824; c) S. Grimme, S. Ehrlich, L. Goerigk, *J. Comput. Chem.* **2011**, *32*, 1456 – 1465; d) F. Weigend, R. Ahlrichs, *Phys. Chem. Chem. Phys.* **2005**, *7*, 3297 – 3305; e) B. Metz, H. Stoll, M. Dolg, *J. Chem. Phys.* **2000**, *113*, 2563 – 2569.
[33] a) A. D. Becke, *J. Chem. Phys.* **1993**, *98*, 1372 – 1377; b) C. Lee, W. Yang, R. G. Parr, *Phys. Rev. B* **1988**, *37*, 785 – 789.
[34] M. von Hopffgarten, G. Frenking, *WIREs Comput. Mol. Sci.* **2012**, *2*, 43 – 62.
[35] R. F. W. Bader in *Atoms in Molecules: A Quantum Theory*, Claredon Press, Oxford, **1990**.
[36] A. E. Reed, L. A. Curtiss, F. Weinhold, *Chem. Rev.* **1988**, *88*, 899 – 926.
[37] A. S. Nizovtsev, A. S. Ivanov, A. I. Boldyrev, S. N. Konchenko, *Eur. J. Inorg. Chem.* **2015**, 5801 – 5807.
[38] a) A. D. Becke, K. E. Edgecombe, *J. Chem. Phys.* **1990**, *92*, 5397 – 5403; b) B. Silvi, A. Savin, *Nature* **1994**, *371*, 683 – 686.
[39] S. Raub, G. Jansen, *Theor. Chem. Acc.* **2001**, *106*, 223 – 232.
[40] C. Schwarzmaier, A. Y. Timoshkin, G. Balázs, M. Scheer, *Angew. Chem. Int. Ed.* **2014**, *53*, 9077 – 9081; *Angew. Chem.* **2014**, *126*, 9223 – 9227.

Received: November 12, 2015
Revised: January 22, 2016
Published online: February 29, 2016

